Interaction of Riluzole with the Closed-Inactivated State of Kv4.3 Channels

Hye Sook Ahn, Sung Eun Kim, Hyun-Jong Jang, Myung-Jun Kim, Duck-Joo Rhie, Shin-Hee Yoon, Yang-Hyeok Jo, Myung-Suk Kim, Ki-Wug Sung and Sang June Hahn

Department of Physiology (H.S.A, S.E.K, H.-J.J., M.-J.K., D.-J.R., S.-H.Y., Y.-H.J., M.-S.K., S.J.H.), Department of Pharmacology (K.-W.S.), Medical Research Center, College of Medicine, The Catholic University of Korea, 505 Banpo-dong, Socho-gu, Seoul 137-701, Korea

a) Running title: Riluzole and Kv4.3

b) Corresponding author:

Sang June Hahn, M.D., Ph.D.
Department of Physiology
College of Medicine
The Catholic University of Korea
505 Banpo-dong, Socho-gu
Seoul 137-701, Korea
Tel: 82-2-590-1170
Fax: 82-2-532-9575
E-mail: sjhahn@catholic.ac.kr

c) The number of text pages, figures and references:

28 text pages

8 figures

40 references

The number of words:

Abstract: 250

Introduction: 439

Discussion: 1603

d) A list of non-standard abbreviations used in the paper:

Kv, voltage-gated K^+ channel; CHO, Chinese hamster ovary; IMDM, Iscoves' modified Dulbecco's medium

ABSTRACT

The effect of riluzole on Kv4.3 was examined using the whole-cell patch-clamp technique. Riluzole inhibited the peak amplitude of Kv4.3 in a reversible, concentration-dependent manner with an IC_{50} of 115.6 μM. Under control conditions, a good fit for the inactivation of Kv4.3 currents to a double exponential function, with the time constants of the fast component (τ_f) and the slow component (τ_s) was obtained. τ_f was not altered by riluzole at concentrations up to 100 μM but τ_s became slower with increasing riluzole concentration, resulting in the cross-over of the currents. The inhibition increased steeply with increasing channel activation at more positive potentials. In the full activation voltage range positive to +30 mV, however, no voltage-dependent inhibition was found. Riluzole shifted the voltage dependence of the steady-state inactivation of Kv4.3 in the hyperpolarizing direction in a concentration-dependent manner. However, the slope factor was not affected by riluzole. The K_i for riluzole for interacting with the inactivated state of Kv4.3 was estimated from the concentration-dependent shift in the steady-state inactivation curve and was determined to be 1.2 μM. Under control conditions, closed-state inactivation was fitted to a single exponential function. Riluzole caused a substantial acceleration in the closed-state inactivation. In the presence of riluzole, the recovery from inactivation was slower than under control conditions. Riluzole induced a significant use-dependent inhibition of Kv4.3. These results suggest that riluzole inhibits Kv4.3 by binding to the closed-inactivated state of the channels and that the unbinding of riluzole occurs from the closed state during depolarization.

Voltage-gated K^+ (Kv) channels are closed in the resting state, but are opened upon membrane depolarization and then inactivated for a wide variety of time courses. These channels are the primary modulators of neuronal excitability by altering the repolarization of action potentials and neuronal firing frequencies. In this respect, the inactivation mechanism involves the fine-tuning of Kv channels activity and plays an important role in the modulation of the temporal pattern of the activity of excitable neurons. The two electrophysiologically different types of Kv channels can be distinguished based on inactivation kinetics: delayed-rectifier and A-type K^+ channels. Kv4.3, one of the major A-type currents, is rapidly activated and inactivated upon depolarization, and is expressed at high levels in brain, heart and smooth muscle (Ohya et al., 1997). This channel is activated at a subthreshold membrane potential, therefore modulating the threshold for the spike generation of neurons (Yuan et al., 2002). Thus, this channel may serve as an important target of certain drugs that are involved in the regulation of neuronal activity.

Riluzole (2-amino-6-trifluoromethoxy benzothiazole) is a neuroprotective agent, and has been shown to be effective in the treatment of convulsion in humans (Bryson et al., 1996; He et al., 2002). The mechanisms of its therapeutic actions have been attributed to the interaction with the inactivated state of voltage-gated Na^+ and Ca^{2+} channels (Benoit and Escande, 1991; Huang et al., 1997; Zona et al., 1998; Urbani and Belluzzi, 2000), and its blocking properties make it a potential candidate used as an anticonvulsant drugs (Romettino et al., 1991; Stutzmann et al., 1991). The actions of riluzole on these channels have been extensively investigated, but relatively little is known concerning its effects on Kv currents, especially on the A-type current. We and others have previously reported that riluzole interacts preferentially with the inactivated

state of Kv1.5, cloned delayed rectifier Kv channels in CHO cells and outward K^+ currents in cultured rat cortical neurons (Zona et al., 1998; Ahn et al., 2005). However, riluzole also modulates several types of K^+ channels by alternate mechanisms (Duprat et al., 2000; Grunnet et al., 2001). For example, riluzole induces the slowing of the inactivation by oxidation of a cysteine in the N-terminal inactivation domain of Kv1.4, another A-type current (Xu et al., 2001). Since Kv channels display a wide variety of time courses and kinetic properties in the inactivation process, an understanding of the modulation of channel inactivation by drugs has been a focus of intense interest. The purpose of the present study was to characterize the action of riluzole on the inactivation kinetics of Kv4.3, and compare its mechanisms of action with those for Kv1.4.

Materials and Methods

Cell cultures. Rat Kv4.3 cDNA was kindly provided by Dr. Y. Imaizumi (Nagoya City University, Japan). The Kv4.3 cDNA was subcloned into a mammalian expression vector, pCR3.1 (Invitrogen Corporation, Grand Island, NY, USA) as previously described (Ohya et al., 1997). CHO cells (ATCC, Rockville, MD, USA) were maintained in Iscoves' modified Dulbecco's medium (IMDM, Invitrogen Corporation) supplemented with 10% fetal bovine serum, 0.1 mM hypoxanthine and 0.01 mM thymidine in a humidified 5% CO_2 incubator at 37°C. Kv4.3 constructs were stably transfected into CHO cells using the lipofectamine reagent (Invitrogen Corporation). The transfected CHO cells in IMDM containing 1 mg/ml of geneticin (Invitrogen Corporation) were incubated for 48 h under a humidified 5% CO_2 incubator at 37°C. The selected cells were cultured in 96 well plates by serial dilution with IMDM containing 0.5 mg/ml of geneticin and stable transfectants were selected by a prolonged culture period. The transfected cells were exchanged with fresh IMDM containing 0.3 mg/ml of geneticin and passed at 2 - 3 day intervals using a brief trypsin-EDTA treatment. The cells were seeded onto glass coverslips (diameter: 12 mm, Fisher Scientific, Pittsburgh, PA, USA) in a 35 mm dish 1 day before use. For the electrophysiological experiments, coverslips with attached cells were transferred to a continually perfused recording chamber (RC-13, Warner Instrument Corporation, Hamden, CT, USA).

Electrophysiological recordings. The patch-clamp was used in the the whole-cell configuration at room temperature (22 - 24°C) using an Axopatch 200B amplifier (Axon Instruments, Union City, CA, USA). Patch pipettes were pulled from a glass capillary

tubing (PG10165-4, World Precision Instruments, Sarasota, FL, USA) using a puller (Model P-97, Sutter Instrument Co., Novato, CA, USA). The tip resistances of the recording pipettes in the bath solution were 2 - 3 MΩ. Series resistances were approximately 4 to 8 MΩ. Whole-cell capacitive currents were compensated with analog compensation. Series resistance compensation (80%) was employed if the current exceeded 1 nA. The currents were low-pass filtered at 2 kHz (four-pole Bessel filter) and sampled at 5 kHz before being digitized. Data acquisition and analysis were performed with an IBM pentium computer, using the pClamp 9.01 software (Axon Instruments).

Solutions and drugs. The bath solution contained: 140 mM NaCl, 5 mM KCl, 1 mM $CaCl_2$, 1 mM $MgCl_2$, and 10 mM HEPES and was adjusted to pH 7.3 with NaOH. The internal pipette solution contained: 140 mM KCl, 1 mM $CaCl_2$, 1 mM $MgCl_2$, 10 mM HEPES, and 10 mM EGTA and was adjusted to pH 7.3 with KOH. The measured osmolarity of the solutions was 300 - 340 mOsm. Riluzole (Tocris Cookson, Bristol, UK) was dissolved in dimethyl sulfoxide to make a 100 mM stock solution and then appropriately diluted with bath solution.

Data Analysis. The Origin 7.0 software program (Microcal Software, Inc., Northampton, MA, USA) was used for the analysis. The concentration-response data were fitted to the following logistic equation:

$$y = 1/[1 + ([D]/IC_{50})^{n}]$$

where IC_{50} is the concentration of riluzole required to produce 50% inhibition, [D] the concentration of riluzole and n the Hill coefficient. Kv4.3 currents were elicited by applying 500 ms depolarizing pulses from a holding potential of -80 mV to +40 mV at 10 s intervals. The voltage dependence for steady-state inactivation was investigated

using a two-pulse voltage protocol; currents were measured by 500 ms depolarizing pulses to +40 mV while 1 s preconditioning pulses were varied from –110 mV to +0 mV stepped by 5 mV at 10 s intervals in the absence and presence of the drug. The resulting steady-state inactivation data were fitted to the Boltzmann equation:

$$(I - I_c)/(I_{max} - I_c) = 1/[1 + \exp(V - V_{1/2})/k]$$

in which I_{max} represents the current measured at the most hyperpolarized preconditioning pulse, I_c a non-zero current which was not inactivated at the most depolarized preconditioning pulse, k the slope factor, V the test potential and $V_{1/2}$ the potential at which the conductance was half-maximal. We eliminated the non-zero residual current by subtracting it from the actual value.

The data are expressed as the mean ± S.E. One-way analysis of variance, followed by Dunnett's test, was used to evaluate the statistical significance of the observed differences. Statistical significance was considered at $p < 0.05$.

JPET Fast Forward. Published on June 30, 2006 as DOI: 10.1124/jpet.106.106724
This article has not been copyedited and formatted. The final version may differ from this version.

RESULTS

Concentration Dependence of Kv4.3 Inhibition. Fig. 1A shows representative recordings of Kv4.3 currents elicited by 500 ms depolarizing pulses to + 40 mV under control conditions and in the presence of different concentrations of riluzole. Under control conditions, Kv4.3 began to become activated at a potential of -30 mV, and was fully activated at +40 mV and then became completely inactivated during the application of depolarizing pulses, as reported previously (Ohya et al., 1997). Thus, a depolarization pulse of +40 mV was used to test the effect of riluzole. Riluzole significantly decreased the peak amplitude of Kv4.3 in a concentration-dependent manner. The concentration-response curve for riluzole on Kv4.3 at + 40 mV is shown in Fig. 1B. The normalized inhibition was plotted as a function of drug concentration, and was fit to a Hill equation, giving an IC_{50} of 115.6 ± 7.6 μM and a Hill coefficient 2.4 ± 0.3 (n = 6). In the present study, riluzole decreased the peak amplitude of Kv4.3 in a concentration-dependent manner, but its most obvious effect appeared to be a decrease in the rate for current decay, resulting in the cross-over of the current traces obtained under control conditions and after the addition of riluzole (Fig. 2A). To study the effect of riluzole on the inactivation kinetics of Kv4.3, the time constants for the inactivation were measured. The time course of inactivation of Kv4.3 at + 40 mV under control conditions was fitted to a double exponential function, with a fast time constant (τ_f) of 14.8 ± 0.3 ms and a slow time constant (τ_s) of 107.6 ± 5.4 ms (n = 6). Riluzole had no effect on the fast inactivation (τ_f) of Kv4.3, but caused a significant decrease in the rate of slow inactivation with a τ_s value of 113.0 ± 6.5 ms, 130.9 ± 10.5 ms and 145.5 ± 9.3 ms for 10, 30 and 100 μM (n = 6, $p < 0.05$), respectively (Fig. 2B). Therefore,

JPET Fast Forward. Published on June 30, 2006 as DOI: 10.1124/jpet.106.106724
This article has not been copyedited and formatted. The final version may differ from this version.

riluzole increased the slow component of inactivation from the control value of 10.3 ± 0.7% to 12.0 ± 0.8%, 14.6 ± 1.1% and 20.6 ± 0.7% (n = 6) for 10, 30 and 100 μM riluzole, respectively. The activation time constants were calculated by fitting a single exponential to the final 50% of activation (Snyders et al., 1993). Under control conditions, the time constant of activation was 0.51 ± 0.06 ms (n = 6). In the presence of riluzole, the time constants of activation were 0.49 ± 0.05 ms and 0.46 ± 0.06 ms (n = 6) for 10 and 30 μM, respectively, indicating that the kinetics of activation were not significantly affected by riluzole.

Voltage Dependence of the Inhibition by Riluzole. Fig. 3A displays current-voltage relationships for Kv4.3 under control conditions and after the application of 100 μM riluzole. Riluzole reduced Kv4.3 at all test potentials where Kv4.3 was activated (Fig. 3B). However, the inhibition of Kv4.3 was larger at more depolarized potentials. To quantify the voltage dependence of Kv4.3 inhibition, the relative currents before and after the application of riluzole were plotted as a function of test potential (Fig. 3C). In the presence of riluzole, the inhibition increased steeply between - 20 and + 20 mV. At a test potential of – 20 mV, riluzole inhibited the Kv4.3 current by 5.7 ± 9.5% (n = 5). This inhibition increased to 39.5 ± 4.7% at + 20 mV (n = 5, $p < 0.05$). Between + 30 and +60 mV where the maximal conductance is reached, however, the degree of inhibition was found to be uniform.

Shift of the Steady-State Inactivation Curves. To assess the effect of riluzole on the voltage dependence of channel availability, steady-state inactivation curves were generated using standard double pulse protocols (Fig. 4A). The data points were fitted to a Boltzmann function in order to estimate $V_{1/2}$ and k. The steady-state inactivation curves for Kv4.3 in the control had $V_{1/2}$ values of -50.7 ± 1.6 mV and k of 4.6 ± 0.3 mV

JPET Fast Forward. Published on June 30, 2006 as DOI: 10.1124/jpet.106.106724
This article has not been copyedited and formatted. The final version may differ from this version.

(n = 8). Riluzole significantly shifted the inactivation curve ($V_{1/2}$) to a hyperpolarized potential in a concentration-dependent manner (-63.3 ± 2.6 mV at 30 μM, -72.3 ± 2.4 mV at 100 μM, n = 8, $p < 0.05$). However, no significant change in k for the curve in the presence of riluzole was found (4.8 ± 0.3 mV at 30 μM, 4.9 ± 0.2 mV at 100 μM, n = 8). Whereas the apparent dissociation constant, K_R, for the riluzole-induced inhibition of Kv4.3 in the closed state can be estimated from the reduction in the peak amplitude of the Kv4.3 current (Fig. 1), the apparent dissociation constant, K_i, for the riluzole-induced inhibition in the inactivated state can be estimated from the concentration-dependent shift in the steady-state inactivation curve (Bean et al., 1983). The theoretical value of K_i was calculated to be 1.2 ± 0.5 μM (n = 8) (Fig. 4B). Thus, the affinity of riluzole for the inactivated state of Kv4.3 is more than 90 times that for closed state.

Interaction with the Closed-Inactivated State. Because previous studies have shown that Kv4.3 channels are predominantly inactivated from the closed state (Beck and Covarrubias, 2001; Wang et al., 2005), we examined the possible effect of riluzole on the kinetics of closed-state inactivation (Fig. 5A). We used subthreshold depolarizing pulses (-60 mV), because the inactivation occurs predominantly from the close state at this holding potential. Under control conditions, a 12 s conditioning pulse to -60 mV inactivated 53.2 ± 4.3% (n = 8) of the Kv4.3 channels (Fig. 5B). The time course for closed-state inactivation was fitted to a single exponential function with a time constant of 4.2 ± 0.5 s (n = 8). In the presence of 100 μM riluzole, the rate of close-stated inactivation was accelerated and inactivation was almost complete after a 1 s conditioning pulse. Closed-state inactivation was also fitted to a single exponential function with a time constant of 0.2 ± 0.03 s (n = 8, $p < 0.05$).

Use-dependent inhibition. The use-dependence of riluzole action was evaluated

with 10 consecutive pulses to +40 mV at 1 and 2 Hz. Under control conditions (Fig. 6A), the Kv4.3 currents displayed a slight decline at 1 Hz (6.2 ± 2.4%, *n* = 6). This percentage increased to 30.2 ± 4.5 % (*n* = 6) at a frequency of 2 Hz. In the presence of 100 μM riluzole, the amplitude of the peak current declined more rapidly with successive pulses, reaching a steady-state level equivalent to 39.4 ± 4.4% of the control after 5 pulses at 1 Hz. The degree of frequency-dependent inhibition increased more markedly at 2 Hz. Thus, the potency of riluzole appears to be enhanced by increasing the frequency of the depolarizing stimulation.

Recovery from Inactivation of Kv4.3. The effects of riluzole on the kinetics of Kv4.3 recovery from steady-state inactivation are shown in Fig. 7A. Under control conditions, the recovery from the inactivation of Kv4.3 was complete after an interpulse interval of 1 s and was best fit to a single exponential function with a time constant of 258.4 ± 25.6 ms (*n* = 6) (Fig. 7B). In the presence of 100 μM riluzole, however, the recovery process was best fit to a biexponential function with a fast time constant of 379.4 ± 51.7 ms and a slow time constant of 2001.6 ± 164.9 ms (*n* = 6). Both time constants differed significantly from the time constant under control conditions (*n* = 6, $p < 0.05$), indicating the slower recovery kinetics of Kv4.3 currents.

Reversibility of the Effects of Riluzole. Fig. 8A shows the results of a typical experiment in which a single pulse to +40 mV was repeated while 100 μM riluzole, separated by washout periods, was applied. Riluzole caused a decrease in the amplitude of Kv4.3 by about 50% within 1 min. The repeated application of riluzole caused the rapid inhibition of Kv4.3 but the peak amplitudes of the current were completely restored to the control values upon washout (Fig. 8B). Riluzole slowed the inactivation kinetics of Kv4.3 slightly (τ_f of 16.2 ± 1.7 ms, τ_s of 116.2 ± 8.6 ms, *n* = 4) after a

washout, but the values were not statistically different from the control values (Fig. 2B), indicating that the effects of riluzole were completely reversible upon washout.

JPET Fast Forward. Published on June 30, 2006 as DOI: 10.1124/jpet.106.106724
This article has not been copyedited and formatted. The final version may differ from this version.

DISCUSSION

The findings herein show that riluzole is a potent inhibitor of the Kv4.3 current which is stably expressed in CHO cells. The inhibition is characterized by a reduction in peak amplitude of Kv4.3 and a concentration-dependent shift in steady-state inactivation curves in the hyperpolarizing direction. These results suggest that the inhibition of Kv4.3 by riluzole is mainly caused by the binding of riluzole to the inactivated state of the channel.

Riluzole is a neuroprotective agent and its mechanism of action may involve, in part, the blocking of voltage-gated Na^+ channels (Taylor and Meldrum, 1995; Doble, 1996). Riluzole also modulates several types of voltage-gated K^+ and Ca^{2+} channels (Huang et al., 1997; Wu and Li, 1999; Duprat et al., 2000; Grunnet et al., 2001; Cao et al., 2002). The most important aspect of the mechanism of blocking voltage-gated ion channels by riluzole is its high affinity for the inactivated state, compared to the closed or open state of the channels (Benoit and Escande, 1991; Huang et al., 1997; Zona et al., 1998; Ahn et al., 2005). In the present study, the following observations suggest that riluzole inhibits Kv4.3 through a preferential interaction with the inactivated state of the channel. First, the voltage dependence of the steady-state inactivation curves was shifted in the hyperpolarizing direction in a concentration-dependent manner. Second, the inhibitory action of riluzole was use-dependent. The reshaping of the recovery kinetics with a slower component may result from the slower dissociation of this drug from its binding site of Kv4.3, which may explain the use-dependent inhibition by riluzole. Third, riluzole produced a voltage-dependent inhibition of Kv4.3 over the voltage range corresponding to channel opening. This voltage-dependence of riluzole inhibition appears to be due to the voltage dependence of inactivation of Kv4.3 currents.

Therefore, our observations confirm that the mechanism by which riluzole inhibits Kv4.3 is similar to those observed for several other delayed rectifier K^+ channels (Zona et al., 1998; Ahn et al., 2005). However, other molecular mechanisms of action have been reported for riluzole. For example, riluzole slows the inactivation of Kv1.4 channels via the oxidation of a cysteine residue in the N-terminal inactivation ball (Xu et al., 2001). Channel inactivation by membrane depolarization prevents the riluzole-induced oxidation of a cysteine in the N-terminal domain of Kv1.4 channels. In the present study, however, the inhibitory effects of riluzole were more pronounced when Kv4.3 channels were inactivated. It is known that Kv1.4 and Kv4.3 are typical A-type currents which are rapidly activated and inactivated during depolarization. These types of channels are expressed primarily in pre- and postsynaptic membranes in central and peripheral neurons (Sheng et al., 1992). Whereas Kv1.4 channels undergo an N-type inactivation (Lee et al., 1996), Kv4.3 channels lack the ball moiety that causes an N-type inactivation, do not follow typical N-type inactivation but include the putative concerted action of the cytoplasmic N- and C- terminal regions (Jerng and Covarrubias, 1997). In addition, while the oxidation of cysteine residues in N-terminal domain affects the inactivation kinetics of Kv1.4 (Ruppersberg et al., 1991b; Stephens et al., 1996), the modulation of inactivation by an oxidation/reduction mechanism has not been reported for Kv4.3 channels. More importantly, whereas the inactivation of Kv1.4 channels occurs only from the open state (Demo and Yellen, 1991), Kv4.3 channels are inactivated from both the open and closed states and can enter the inactivated state directly from closed states without activation (Beck and Covarrubias, 2001; Wang et al., 2005). Thus, the previous observations are extended and clarified by demonstrating that riluzole binds preferentially to the closed-inactivated states.

Another characteristic of the riluzole-induced inhibition of Kv4.3 was that the peak amplitude of the Kv4.3 currents was reduced and the subsequent inactivation of the current was slowed, resulting in the cross-over of the current traces obtained under control conditions and after the addition of riluzole. The instantaneous inhibition at the onset of a depolarizing pulse could be attributed to an interaction of riluzole with the closed state of the Kv4.3 channel. While the fast inactivation time course for Kv4.3 was not altered by riluzole, the slow time course was slowed substantially. One possible explanation is that the slowing of inactivation could also due to delayed activation and inactivation. These effects have been described in A-type current I_{to} with a similar mode (Campbell et al., 1993). In ferret ventricular myocytes, 4-AP not only reduced the peak amplitude of I_{to} but also slowed the apparent rate of both the activation and inactivation processes, resulting in the cross-over of the current. These results suggest that 4-AP inhibits I_{to} through a closed state blocking mechanism. Because the activation kinetics were not affected by riluzole in the present study, the rate at which channels are delivered to the open state from the closed state was slowed due to delayed drug dissociation. Thus, riluzole must unbind from the closed channel during the late phase of the depolarizing pulse, and the channel enters into the open state after the dissociation of the drug and inactivates at a normal rate, which led to a cross-over phenomenon. Similar results have been reported for 4-AP on Kv4.2 (Kirsch et al., 1986) and EGCG on Kv1.5 (Choi et al., 2001): the closed state inhibition can be relieved during membrane depolarization due to the unbinding of the drug from the channel at depolarized potentials. Because Kv4.3 channels can enter the inactivated state directly from the closed state bypassing the open state during subthreshold depolarization (Beck and Covarrubias, 2001; Wang et al., 2005), riluzole interacts with both the closed and

closed-inactivated states of the channel. The binding of riluzole to the closed and closed-inactivated states which contribute to a reduction in the total channel availability for the activation of Kv4.3 caused a decrease in the peak amplitude of the Kv4.3 currents upon depolarization. Thus, a reduction in the peak Kv4.3 current reflects the sum of the inhibition of the closed and closed-inactivated states. Although reopening from inactivation during recovery has been reported for Kv1.4 (Ruppersberg et al., 1991a), the inactivated state of Kv4.3 is generally thought to be an absorbing state and recovers by directly bypassing the open state (Bahring et al., 2001; Beck and Covarrubias, 2001). After riluzole dissociates from the closed or closed-inactivated states during depolarization, Kv4.3 channels can open mainly from the closed state, but not from the closed-inactivated state without deactivation at the hyperpolarized membrane potential, as is the case for Na^+ channels (Kuo and Bean, 1994). Thus, these results suggest that the mechanism of slowing of the inactivation kinetics by riluzole involves a reversal of closed channel inhibition during membrane depolarization.

Based on the shift in steady-state inactivation curves, we estimated the K_i for binding to inactivated channels to be 1.2 μM. Thus, the affinity of riluzole for the inactivated state appears to be more than 90 times higher than that for the closed state. At the recommended daily dose, the average plasma levels of riluzole are in the range between 1-2 μM (Le Liboux et al., 1997). The K_i of 1.2 μM for the inactivated state of Kv4.3 is comparable to the previously reported value for blocking the inactivated Na^+ channels in rat cortical neurons (Urbani and Belluzzi, 2000) and this concentration can easily be reached in brain tissue. A-type K^+ channels are expressed in a wide variety of neurons throughout the central nervous system. In general, this type of current appears to play a prominent role in the regulation of the duration and frequency of the action

JPET Fast Forward. Published on June 30, 2006 as DOI: 10.1124/jpet.106.106724
This article has not been copyedited and formatted. The final version may differ from this version.

potential and neuronal firing pattern. Kv4.3 is primarily expressed in the soma and dendrites of neurons (Serodio and Rudy, 1998), and is activated at subthreshold membrane potentials, thus limiting the back-propagation of the action potential into dendrites and regulating membrane excitability in the hippocampus (Yuan et al., 2002). For example, the inhibition of dendritic A-type channels can modulate the action potential threshold and increase dendritic excitability and the back-propagation of the action potential in the dendrites of hippocampal pyramidal neurons (Hoffman and Johnston, 1998). Therefore, effect of riluzole on Kv4.3 channels observed in the present study could affect the neuronal excitability, which would be adverse to the neuroprotective action of the drug. However, correlating experimental data with clinical implications must proceed with great caution, because riluzole is a non-selective ion channel inhibitor and affects several other ionic currents that are responsible for the configuration of the action potentials. The overall effects of riluzole on neuronal excitability are determined by the sum of the complex interactions of the drug with multiple ion channels through different neuronal membranes. In fact, riluzole decreases current-evoked firing discharge in striatal spiny (Centonze et al., 1998) and cortical neurons (Urbani and Belluzzi, 2000), consistent with the use of this drug as a neuroprotective agent. It should also be noted that the pore-forming α -subunit of the Kv4.3 channel protein by itself can form a voltage-gated K^+ channel in heterologous expression systems but Kv4.3 co-assembles with a large variety of auxiliary subunits, including K^+ channel interacting proteins (KChIPs) in native cells. The interaction of these proteins alters the biophysical properties and drug sensitivity of Kv4.3 channels (Beck et al., 2002; Bett et al., 2006). Thus, the Kv4.3 currents expressed in CHO cells were kinetically and pharmacologically different from the native A-type current. Further

studies are clearly needed to clarify the mechanisms underlying the modulation of riluzole's sensitivity of Kv4.3 by KChIPs.

In conclusion, the results reported herein are consistent with general mechanisms in which riluzole binds to the inactivated state of Kv4.3 channels and thus provides further information on the mechanism of action of this drug, in that it interacts preferentially with the closed-inactivated state of this type channel.

Acknowledgements

We thank Dr. Imaizumi (Department of Molecular and Cellular Pharmacology, Nagoya City University, Japan) for the Kv4.3 cDNA.

JPET Fast Forward. Published on June 30, 2006 as DOI: 10.1124/jpet.106.106724
This article has not been copyedited and formatted. The final version may differ from this version.

References

Ahn HS, Choi JS, Choi BH, Kim MJ, Rhie DJ, Yoon SH, Jo YH, Kim MS, Sung KW and Hahn SJ (2005) Inhibition of the cloned delayed rectifier K+ channels, Kv1.5 and Kv3.1, by riluzole. *Neuroscience* **133**:1007-1019.

Bahring R, Boland LM, Varghese A, Gebauer M and Pongs O (2001) Kinetic analysis of open- and closed-state inactivation transitions in human Kv4.2 A-type potassium channels. *J Physiol* **535**:65-81.

Bean BP, Cohen CJ and Tsien RW (1983) Lidocaine block of cardiac sodium channels. *J Gen Physiol* **81**:613-642.

Beck EJ, Bowlby M, An WF, Rhodes KJ and Covarrubias M (2002) Remodelling inactivation gating of Kv4 channels by KChIP1, a small-molecular-weight calcium-binding protein. *J Physiol* **538**:691-706.

Beck EJ and Covarrubias M (2001) Kv4 channels exhibit modulation of closed-state inactivation in inside-out patches. *Biophys J* **81**:867-883.

Benoit E and Escande D (1991) Riluzole specifically blocks inactivated Na channels in myelinated nerve fibre. *Pflugers Arch* **419**:603-609.

Bett GC, Morales MJ, Strauss HC and Rasmusson RL (2006) KChIP2b modulates the affinity and use-dependent block of Kv4.3 by nifedipine. *Biochem Biophys Res Commun* **340**:1167-1177.

Bryson HM, Fulton B and Benfield P (1996) Riluzole. A review of its pharmacodynamic and pharmacokinetic properties and therapeutic potential in amyotrophic lateral sclerosis. *Drugs* **52**:549-563.

Campbell DL, Qu Y, Rasmusson RL and Strauss HC (1993) The calcium-independent transient outward potassium current in isolated ferret right ventricular myocytes. II. Closed state reverse use-dependent block by 4-aminopyridine. *J Gen Physiol* **101**:603-626.

Cao YJ, Dreixler JC, Couey JJ and Houamed KM (2002) Modulation of recombinant and native neuronal SK channels by the neuroprotective drug riluzole. *Eur J Pharmacol* **449**:47-54.

Centonze D, Calabresi P, Pisani A, Marinelli S, Marfia GA and Bernardi G (1998) Electrophysiology of the neuroprotective agent riluzole on striatal spiny neurons. *Neuropharmacology* **37**:1063-1070.

Choi BH, Choi JS, Min DS, Yoon SH, Rhie DJ, Jo YH, Kim MS and Hahn SJ (2001) Effects of (-)-epigallocatechin-3-gallate, the main component of green tea, on the cloned rat brain Kv1.5 potassium channels. *Biochem Pharmacol* **62**:527-535.

Demo SD and Yellen G (1991) The inactivation gate of the Shaker K+ channel behaves like an open-channel blocker. *Neuron* **7**:743-753.

Doble A (1996) The pharmacology and mechanism of action of riluzole. *Neurology* **47**:S233-241.

Duprat F, Lesage F, Patel AJ, Fink M, Romey G and Lazdunski M (2000) The neuroprotective agent riluzole activates the two P domain K(+) channels TREK-1 and TRAAK. *Mol Pharmacol*

57:906-912.

Grunnet M, Jespersen T, Angelo K, Frokjaer-Jensen C, Klaerke DA, Olesen SP and Jensen BS (2001) Pharmacological modulation of SK3 channels. *Neuropharmacology* **40**:879-887.

He Y, Benz A, Fu T, Wang M, Covey DF, Zorumski CF and Mennerick S (2002) Neuroprotective agent riluzole potentiates postsynaptic GABA(A) receptor function. *Neuropharmacology* **42**:199-209.

Hoffman DA and Johnston D (1998) Downregulation of transient K+ channels in dendrites of hippocampal CA1 pyramidal neurons by activation of PKA and PKC. *J Neurosci* **18**:3521-3528.

Huang CS, Song JH, Nagata K, Yeh JZ and Narahashi T (1997) Effects of the neuroprotective agent riluzole on the high voltage-activated calcium channels of rat dorsal root ganglion neurons. *J Pharmacol Exp Ther* **282**:1280-1290.

Jerng HH and Covarrubias M (1997) K+ channel inactivation mediated by the concerted action of the cytoplasmic N- and C-terminal domains. *Biophys J* **72**:163-174.

Kirsch GE, Yeh JZ and Oxford GS (1986) Modulation of aminopyridine block of potassium currents in squid axon. *Biophys J* **50**:637-644.

Kuo CC and Bean BP (1994) Na+ channels must deactivate to recover from inactivation. *Neuron* **12**:819-829.

Le Liboux A, Lefebvre P, Le Roux Y, Truffinet P, Aubeneau M, Kirkesseli S and Montay G (1997) Single- and multiple-dose pharmacokinetics of riluzole in white subjects. *J Clin Pharmacol* **37**:820-827.

Lee TE, Philipson LH and Nelson DJ (1996) N-type inactivation in the mammalian Shaker K+ channel Kv1.4. *J Membr Biol* **151**:225-235.

Ohya S, Tanaka M, Oku T, Asai Y, Watanabe M, Giles WR and Imaizumi Y (1997) Molecular cloning and tissue distribution of an alternatively spliced variant of an A-type K+ channel alpha-subunit, Kv4.3 in the rat. *FEBS Lett* **420**:47-53.

Romettino S, Lazdunski M and Gottesmann C (1991) Anticonvulsant and sleep-waking influences of riluzole in a rat model of absence epilepsy. *Eur J Pharmacol* **199**:371-373.

Ruppersberg JP, Frank R, Pongs O and Stocker M (1991a) Cloned neuronal IK(A) channels reopen during recovery from inactivation. *Nature* **353**:657-660.

Ruppersberg JP, Stocker M, Pongs O, Heinemann SH, Frank R and Koenen M (1991b) Regulation of fast inactivation of cloned mammalian IK(A) channels by cysteine oxidation. *Nature* **352**:711-714.

Serodio P and Rudy B (1998) Differential expression of Kv4 K+ channel subunits mediating subthreshold transient K+ (A-type) currents in rat brain. *J Neurophysiol* **79**:1081-1091.

Sheng M, Tsaur ML, Jan YN and Jan LY (1992) Subcellular segregation of two A-type K+ channel proteins in rat central neurons. *Neuron* **9**:271-284.

Snyders DJ, Tamkun MM and Bennett PB (1993) A rapidly activating and slowly inactivating potassium channel cloned from human heart. Functional analysis after stable mammalian cell culture expression. *J Gen Physiol* **101**:513-543.

Stephens GJ, Owen DG and Robertson B (1996) Cysteine-modifying reagents alter the gating of the rat cloned potassium channel Kv1.4. *Pflugers Arch* **431**:435-442.

Stutzmann JM, Bohme GA, Gandolfo G, Gottesmann C, Lafforgue J, Blanchard JC, Laduron PM and Lazdunski M (1991) Riluzole prevents hyperexcitability produced by the mast cell degranulating peptide and dendrotoxin I in the rat. *Eur J Pharmacol* **193**:223-229.

Taylor CP and Meldrum BS (1995) Na+ channels as targets for neuroprotective drugs. *Trends Pharmacol Sci* **16**:309-316.

Urbani A and Belluzzi O (2000) Riluzole inhibits the persistent sodium current in mammalian CNS neurons. *Eur J Neurosci* **12**:3567-3574.

Wang S, Bondarenko VE, Qu YJ, Bett GC, Morales MJ, Rasmusson RL and Strauss HC (2005) Time- and voltage-dependent components of Kv4.3 inactivation. *Biophys J* **89**:3026-3041.

Wu SN and Li HF (1999) Characterization of riluzole-induced stimulation of large-conductance calcium-activated potassium channels in rat pituitary GH3 cells. *J Investig Med* **47**:484-495.

Xu L, Enyeart JA and Enyeart JJ (2001) Neuroprotective agent riluzole dramatically slows inactivation of Kv1.4 potassium channels by a voltage-dependent oxidative mechanism. *J Pharmacol Exp Ther* **299**:227-237.

Yuan LL, Adams JP, Swank M, Sweatt JD and Johnston D (2002) Protein kinase modulation of dendritic K+ channels in hippocampus involves a mitogen-activated protein kinase pathway. *J Neurosci* **22**:4860-4868.

Zona C, Siniscalchi A, Mercuri NB and Bernardi G (1998) Riluzole interacts with voltage-activated sodium and potassium currents in cultured rat cortical neurons. *Neuroscience* **85**:931-938.

Footnotes

a) This work was supported by a grant from the Medical Research Center, Korea Science and Engineering Foundation, Republic of Korea (R13-2002-005-01002-0).

b) Send reprint requests to:

Sang June Hahn, M.D., Ph.D.
Department of Physiology
College of Medicine
The Catholic University of Korea
505 Banpo-dong, Socho-gu
Seoul 137-701, Korea
Tel: 82-2-590-1170
Fax: 82-2-532-9575
E-mail: sjhahn@catholic.ac.kr

JPET Fast Forward. Published on June 30, 2006 as DOI: 10.1124/jpet.106.106724
This article has not been copyedited and formatted. The final version may differ from this version.

Legends for Figures

Fig. 1. Concentration-dependence for the riluzole-induced inhibition of Kv4.3 whole-cell currents expressed in CHO cells. (A) Kv4.3 currents were obtained by applying 500 ms depolarizing pulses from a holding potential of −80 mV to +40 mV at 10 s intervals in the absence and presence of 10, 30, 100 and 300 μM riluzole. The dotted line indicates the zero-current level. (B) Concentration-response curve for the inhibition of Kv4.3 currents by riluzole. The peak current of a depolarizing pulse was normalized to the current recorded under control conditions. The normalized currents were plotted against riluzole concentrations, and fitted to the Hill equation. The data yielded an IC_{50} value of 115.6 ± 7.6 μM and a Hill coefficient of 2.4 ± 0.3 for riluzole (n = 6). Data are expressed as means ± S.E.

Fig. 2. Effects of riluzole on the kinetics of inactivation of Kv4.3 currents. (A) Kv4.3 currents in CHO cells were recorded at +40 mV during a 500 ms depolarizing pulse before and after the application of riluzole. In the absence of the drug, the inactivation process was fitted to a double exponential function. In the presence of 10, 30 and 100 μM riluzole, the peak amplitude of Kv4.3 decreased in a concentration-dependent manner and the subsequent time course of inactivation was significantly slowed. As a result, a cross-over phenomenon was observed. The dotted lines indicate the zero-current level. (B) The values for the inactivation time constants of the fast component (τ_f) and the slow component (τ_s) were obtained from a double exponential fit. Statistical significance vs control is indicated by * $p < 0.05$ (n = 6). Data are expressed as means ± S.E.

Fig. 3. Effects of riluzole on the Kv4.3 current-voltage relationship. (A) Representative whole-cell Kv4.3 current traces under control conditions and in the presence of 100 μM riluzole. Whole-cell currents were evoked at 500 ms depolarizing pulses from –80 mV to +60 mV in steps of 10 mV every 10 s from a holding potential of –80 mV in the absence and presence of 100 μM riluzole. (B) Current-voltage curves for riluzole-induced Kv4.3 currents. The data were taken at the peak of depolarizing pulses shown in Fig. 3A under control conditions and after the addition of 100 μM riluzole. (C) Voltage independent inhibition of Kv4.3 currents by riluzole was expressed as a relative current ($I_{Riluzole}/I_{Control}$). The peak amplitude of currents in the presence of riluzole was normalized to that at each voltage in the absence. In the voltage range between -20 and +20 mV for channel opening, the inhibition of Kv4.3 currents by riluzole increased steeply and was significantly different (n = 5, * $p < 0.05$ versus data at -20 mV). The dotted line represents the activation curve of Kv4.3 under control conditions: $V_{1/2}$ and k are -11.5 ± 0.7 mV and 11.1 ± 0.3 mV, respectively (n = 5). Data are expressed as means ± S.E.

Fig. 4. Riluzole produces a negative shift in the steady-state inactivation of Kv4.3. (A) The prepulse inactivation protocol consisted of a sequence of two pulses. The currents were evoked by a 1 s prepulse that was varied from -110 mV to 0 mV stepped by 5 mV and a 500 ms depolarizing pulse to +40 mV in the absence and presence of riluzole. Steady-state inactivation curves are shown as a plot of normalized peak currents during the test pulse as a function of the conditioning potential. The curves represent the best-fit Boltzmann distributions (n = 8). (B) Plot of exp (ΔV/k) against riluzole concentration.

The half-inactivate potential ($V_{1/2}$) and slope factor (k) were obtained from the inactivation curves. The concentration-dependent shift of the midpoint (ΔV) was determined as the difference between $V_{1/2}$ values in control conditions and at 30 and 100 μM concentrations of riluzole. The solid line represents the linear fit to the data. The K_i , the reciprocal of the slope, estimated from this fit was 1.2 ± 0.5 μM (n = 8). Data are expressed as means ± S.E.

Fig. 5. Effects of riluzole on the kinetics of Kv4.3 closed-state inactivation. (A) Kv4.3 currents were recorded at +40 mV using a double-pulse protocol with a conditioning pulse to -60 mV of variable duration. The initial control pulse and conditioning pulse were applied from a membrane potential of -100 mV. (B) The current amplitudes evoked by the second pulse, relative to the amplitude obtained by the initial control pulse, were plotted against the duration of the conditioning pulse. The data were fit well to a single-exponential function (n = 8). Data are expressed as means ± S.E.

Fig. 6. Use-dependent inhibition of Kv4.3 currents by riluzole. (A) Repetitive 200 ms depolarizing pulses of +40 mV from a holding potential of –80 mV were applied at two different frequencies, 1 and 2 Hz under control conditions and after the application of 100 μM riluzole. The dotted lines indicate the zero-current level. (B) The peak amplitudes of current at each pulse were normalized to that of the current obtained at the first pulse and then plotted versus pulse number (n = 6). Data are expressed as means ± S.E.

Fig. 7. Riluzole slowed Kv4.3 recovery from inactivation. A double pulse protocol was

used to characterize the recovery of Kv4.3 channels from inactivation: the first prepulse of a 500 ms depolarizing pulse of +40 mV from a holding potential of -80 mV was followed by a second identical pulse after increasing the interpulse intervals between 50 and 10,000 ms at -80 mV. (A) Typical Kv4.3 current traces for recovery from inactivation were shown under control conditions and in the presence of 100 μM riluzole. (B) Time course of recovery from inactivation. The peak currents elicited by the second test pulse were divided by those evoked by the first prepulse and the normalized data were plotted against the interpulse interval. The plotted data were fit well to a single exponential function under control conditions and a biexponential function in the presence of riluzole (n = 6). Data are expressed as means ± S.E.

Fig. 8. Reversible inhibition of Kv4.3 currents by riluzole. (A) Whole-cell currents were evoked by 500 ms depolarizing pulses of +40 mV from a holding potential of –80 mV at 10 s intervals. The dotted line indicates the zero-current level. (B) Time course of inhibition in the presence of 100 μM riluzole. The peak amplitudes of the currents were plotted as a function of time. The bars indicate the time of application of riluzole.

JPET Fast Forward. Published on June 30, 2006 as DOI: 10.1124/jpet.106.106724
This article has not been copyedited and formatted. The final version may differ from this version.

A

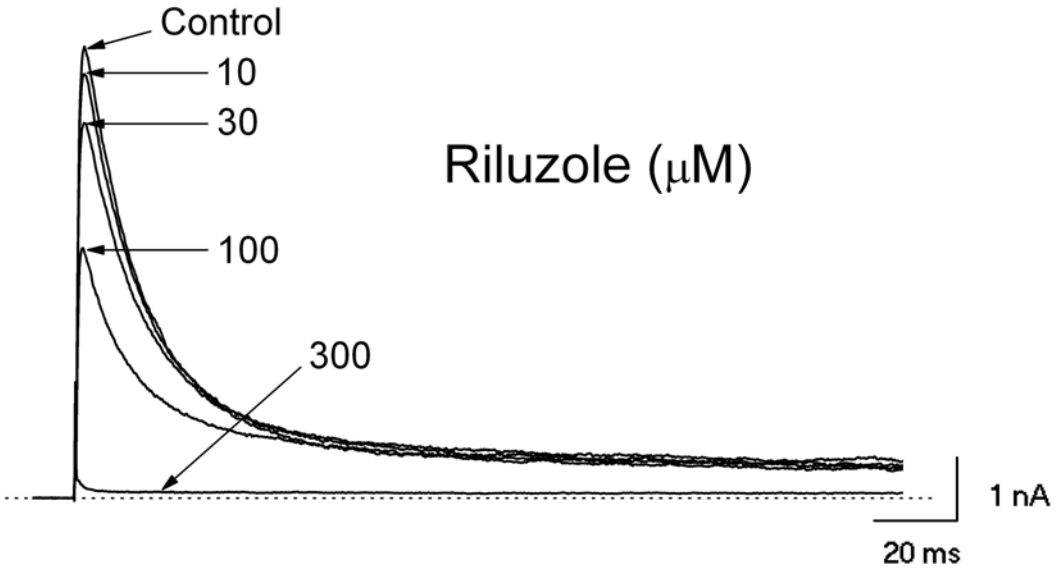

B

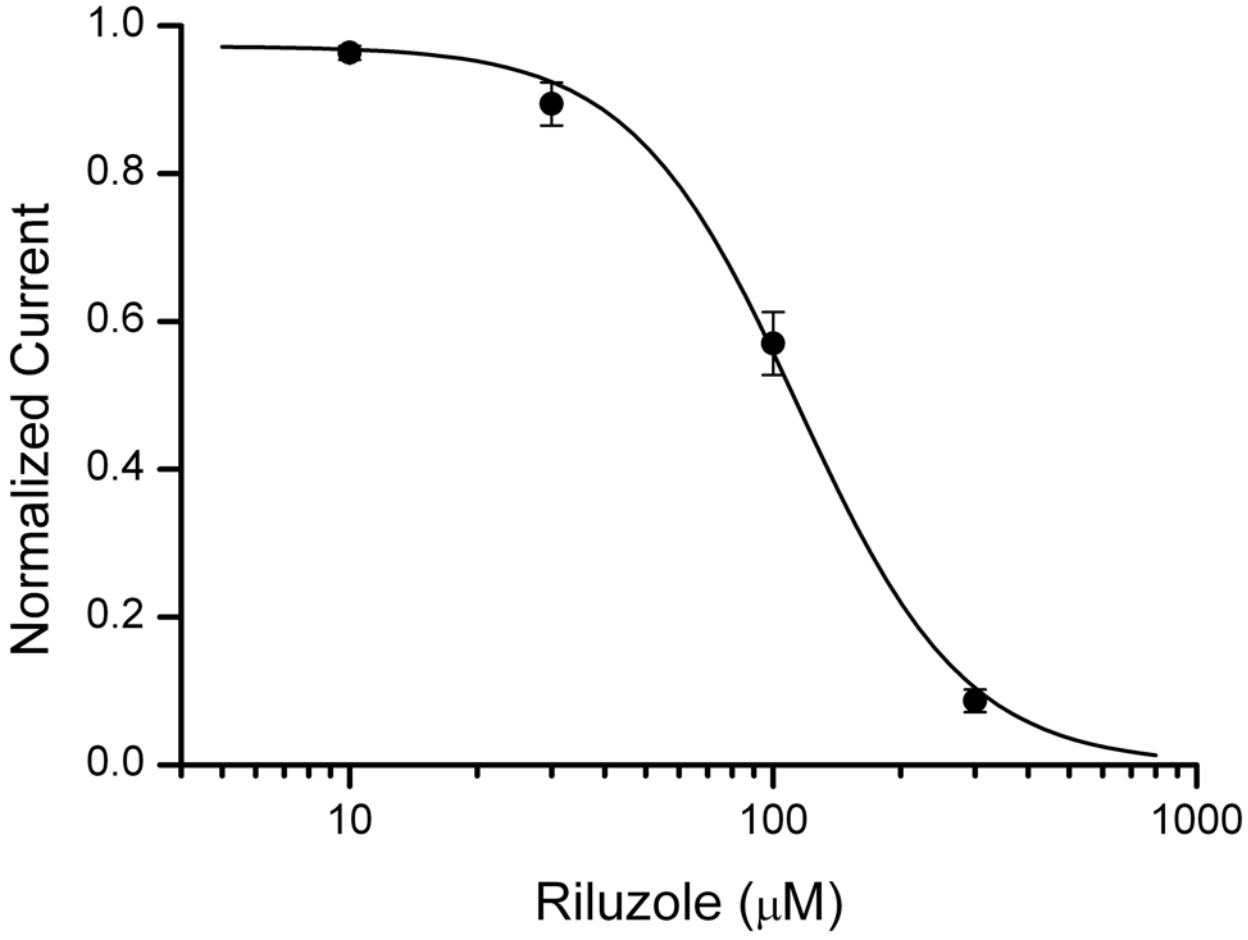

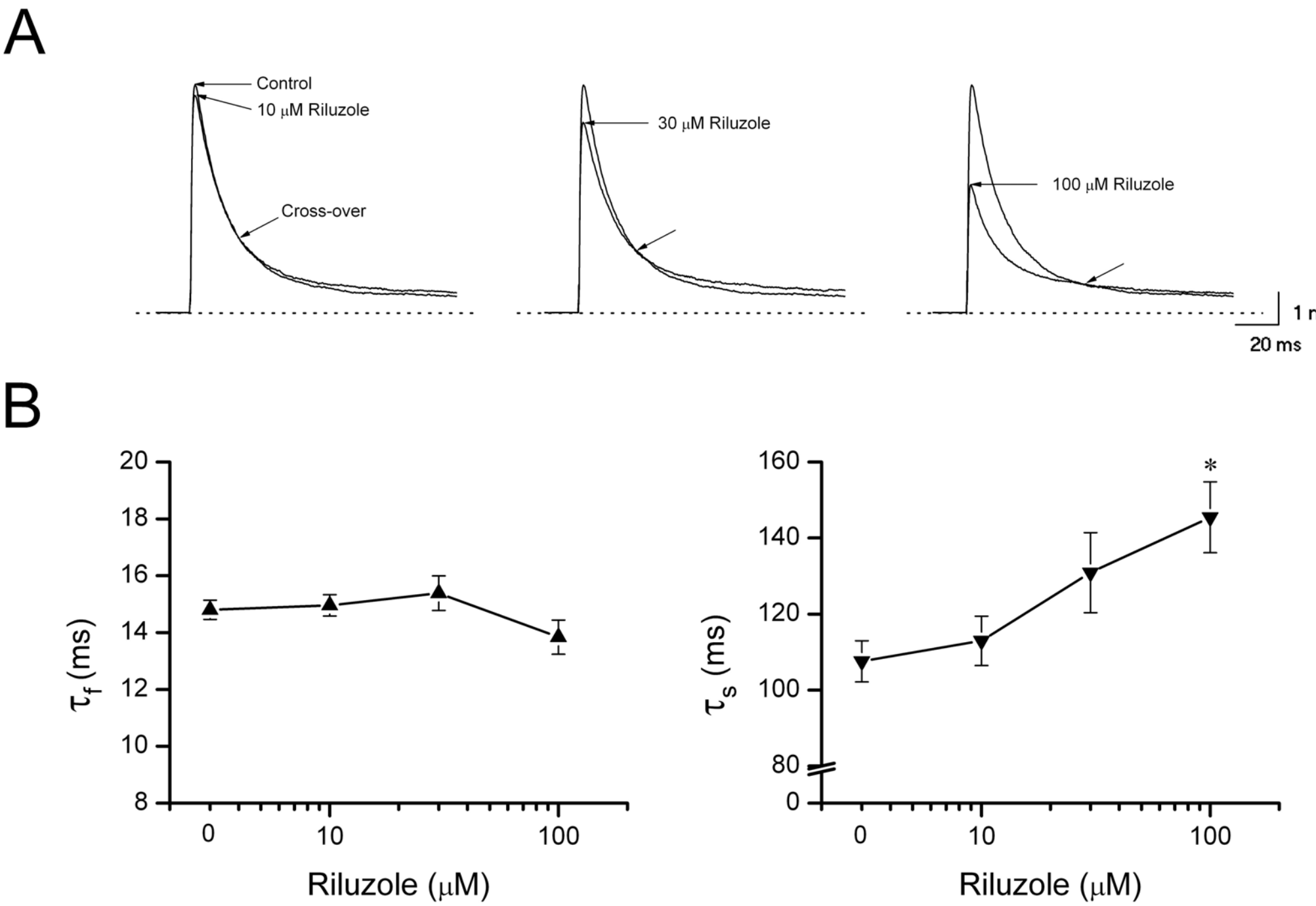

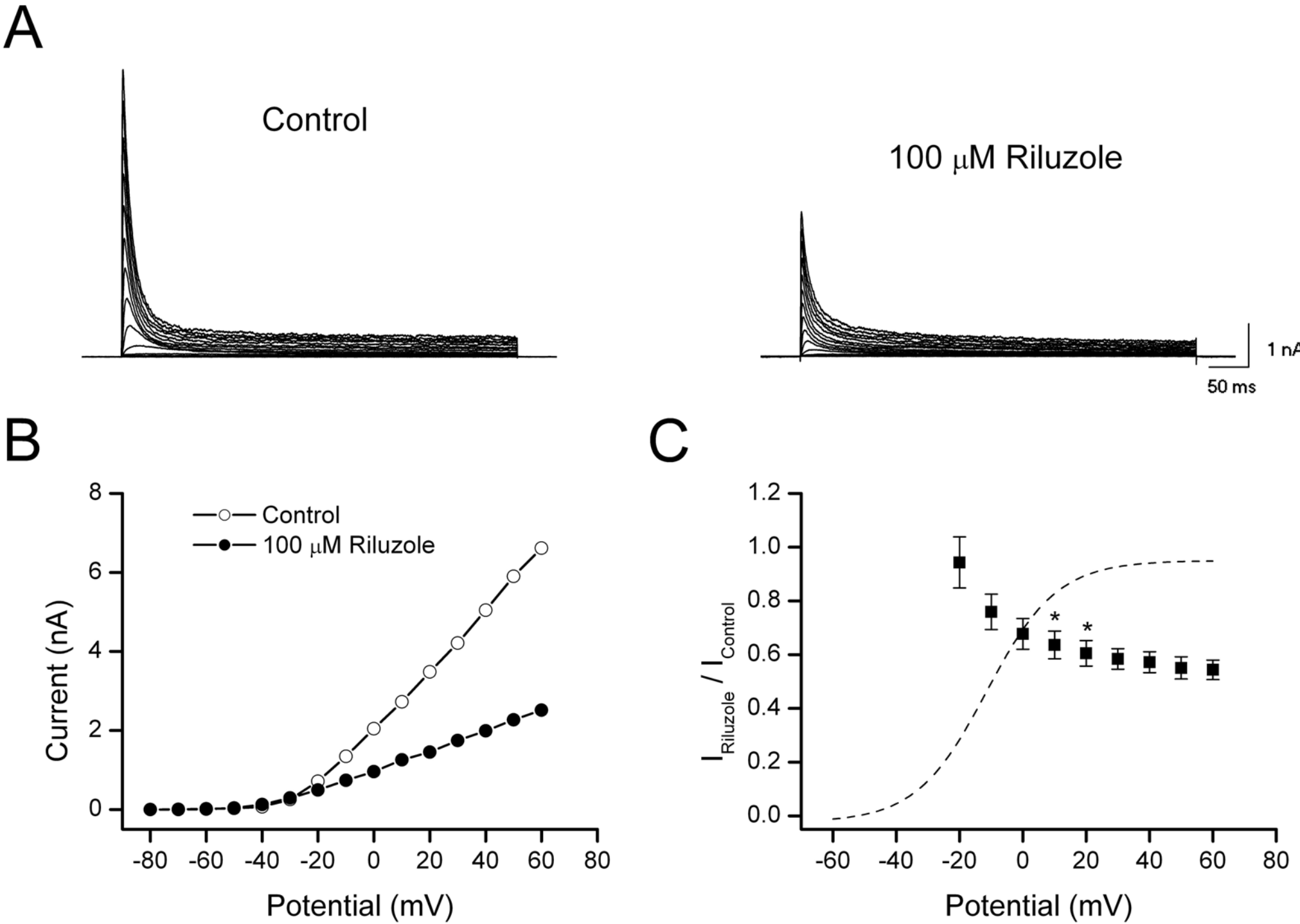

JPET Fast Forward. Published on June 30, 2006 as DOI: 10.1124/jpet.106.106724
This article has not been copyedited and formatted. The final version may differ from this version.

A

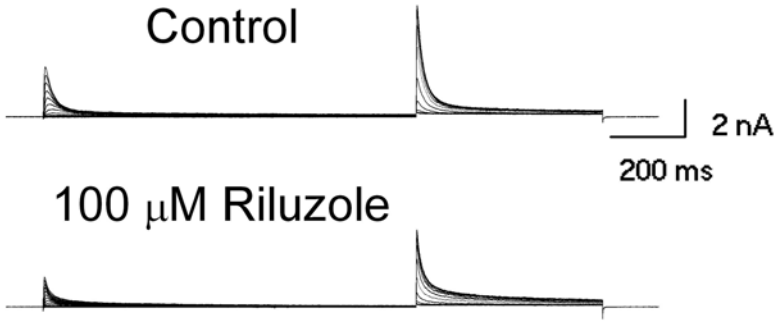

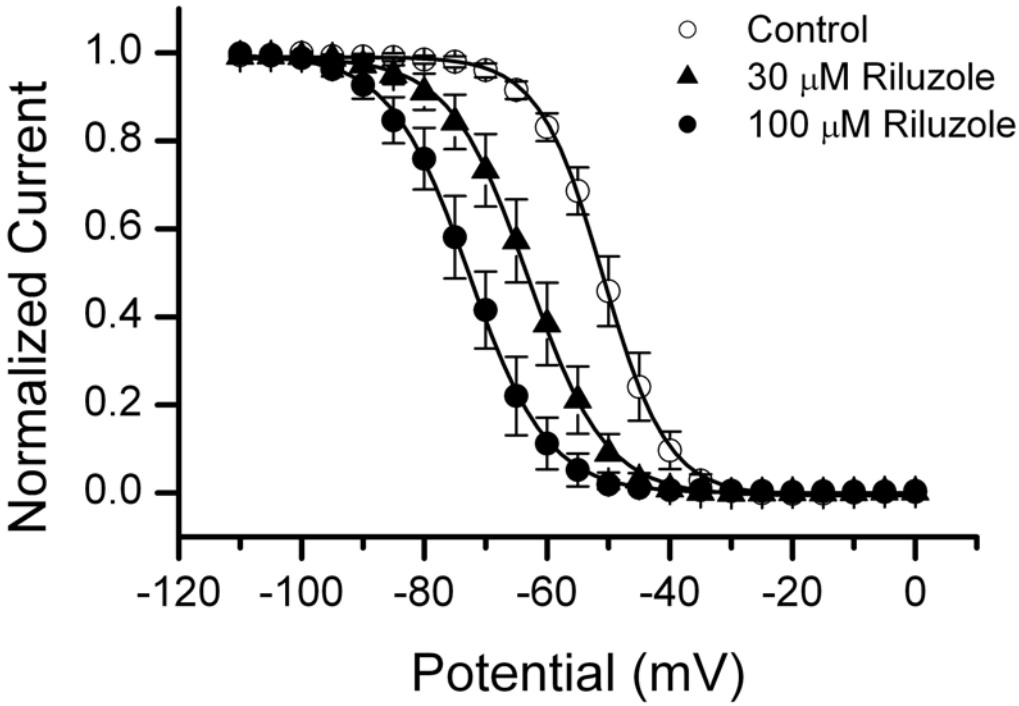

B

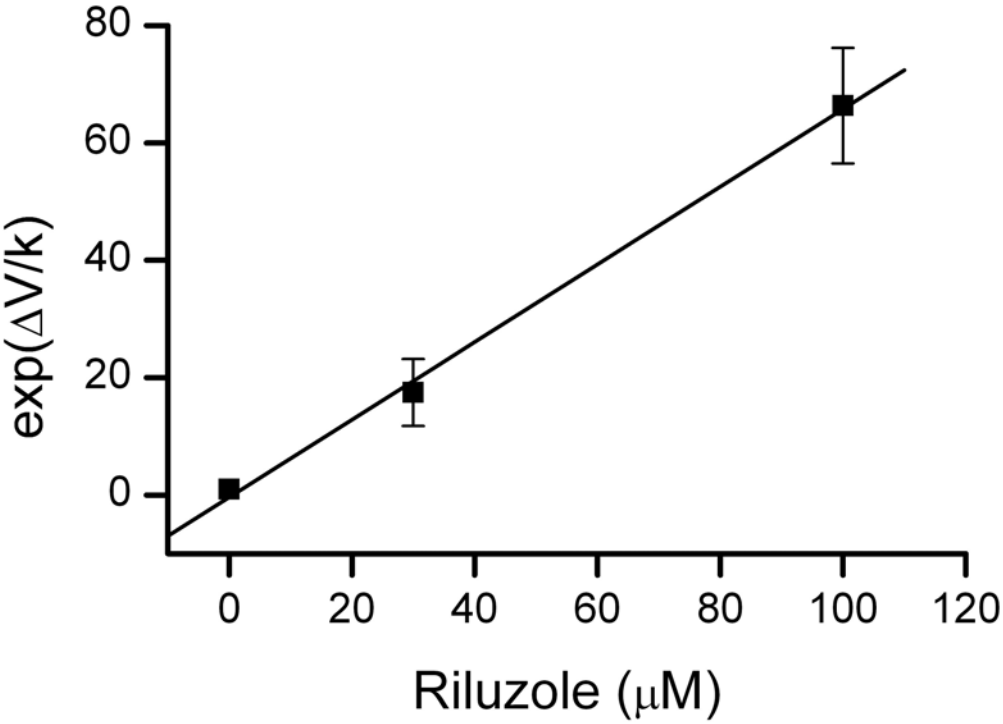

JPET Fast Forward. Published on June 30, 2006 as DOI: 10.1124/jpet.106.106724
This article has not been copyedited and formatted. The final version may differ from this version.

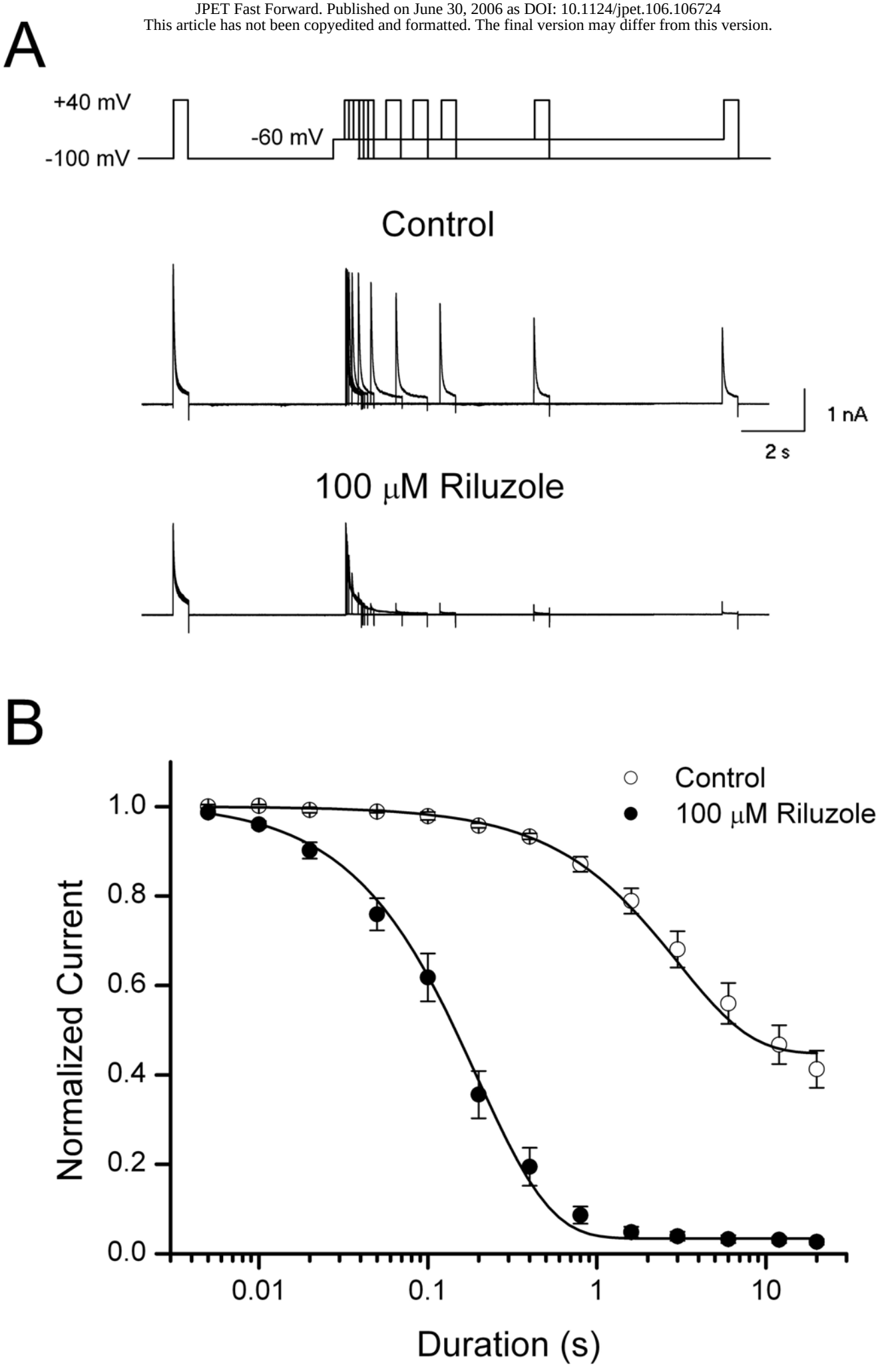

JPET Fast Forward. Published on June 30, 2006 as DOI: 10.1124/jpet.106.106724
This article has not been copyedited and formatted. The final version may differ from this version.

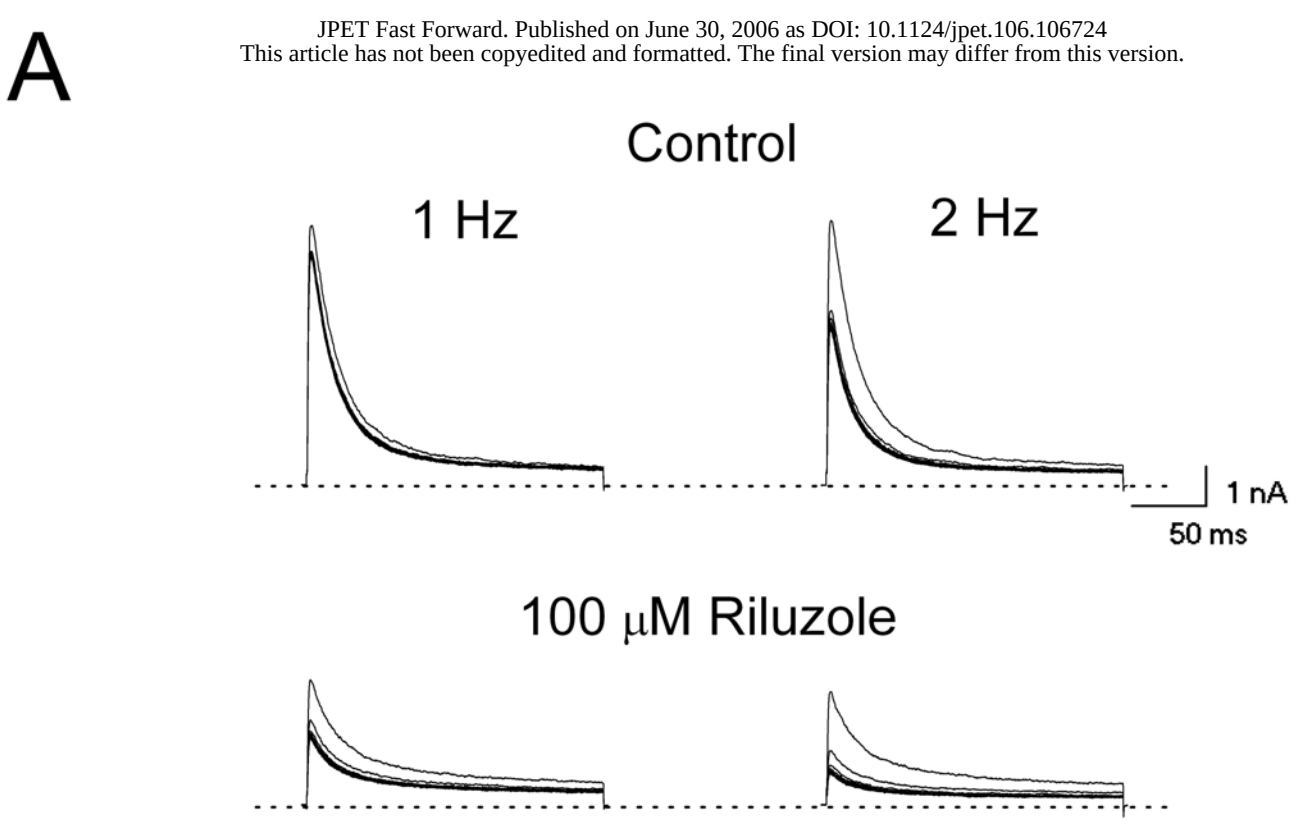

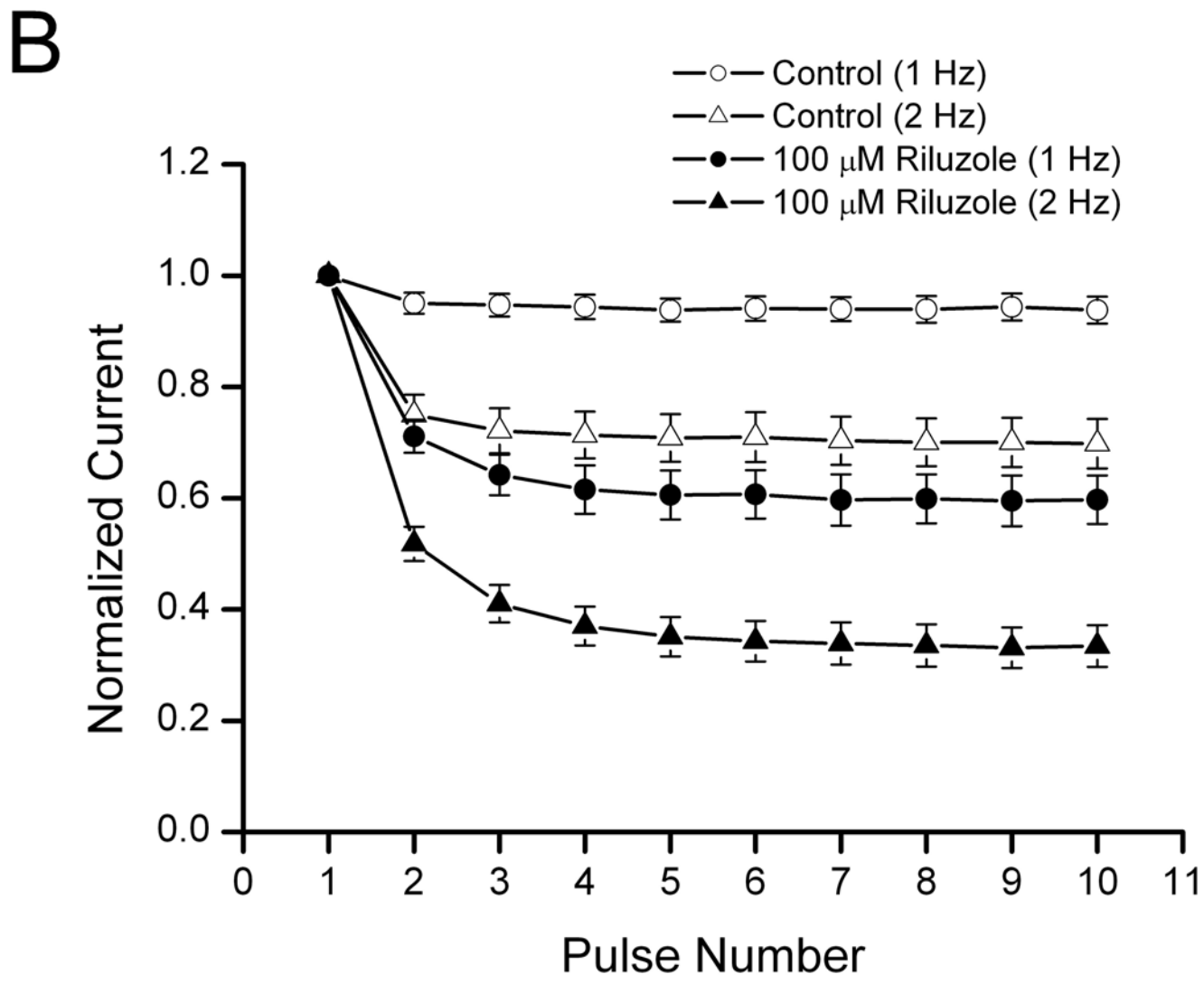

JPET Fast Forward. Published on June 30, 2006 as DOI: 10.1124/jpet.106.106724
This article has not been copyedited and formatted. The final version may differ from this version.

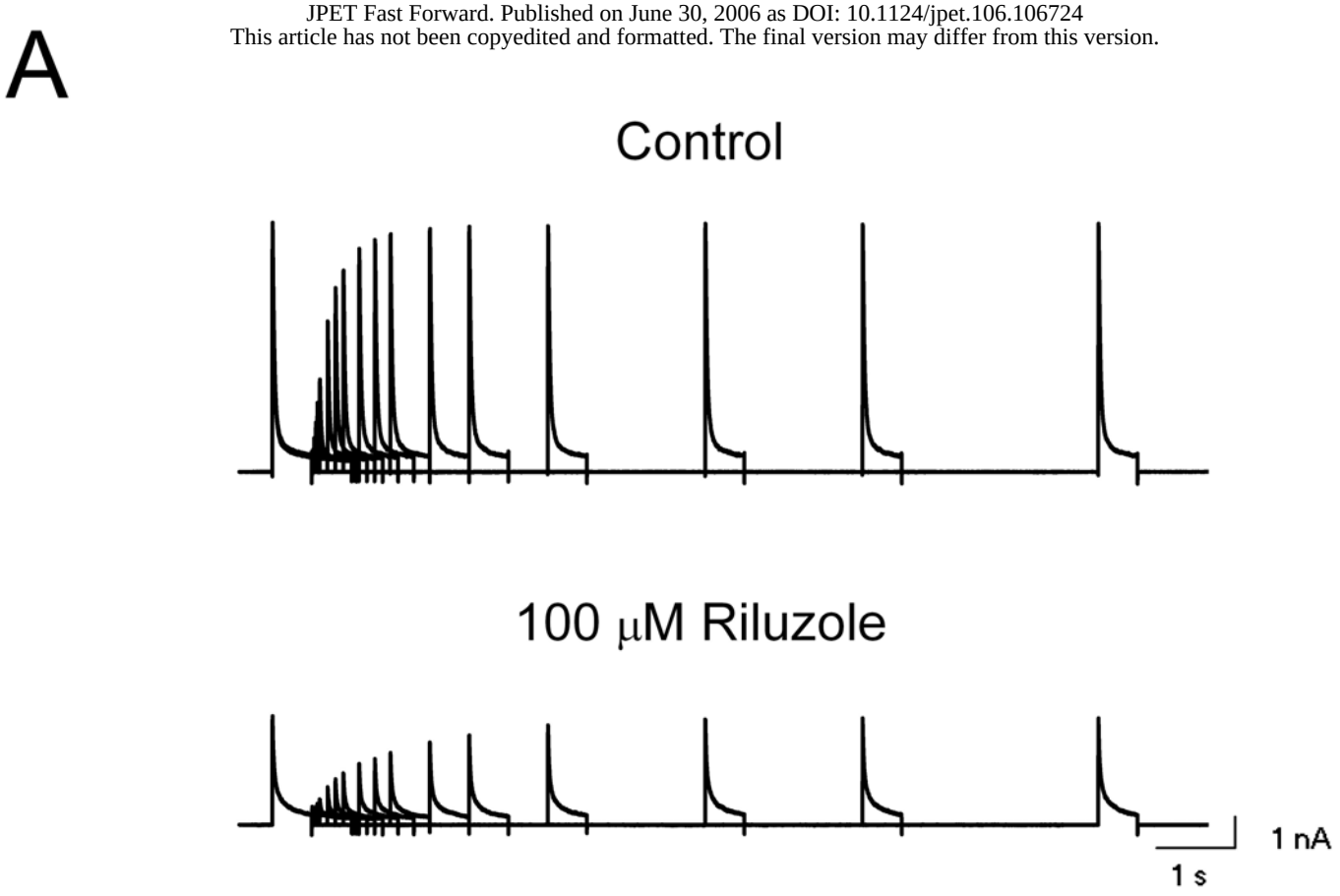

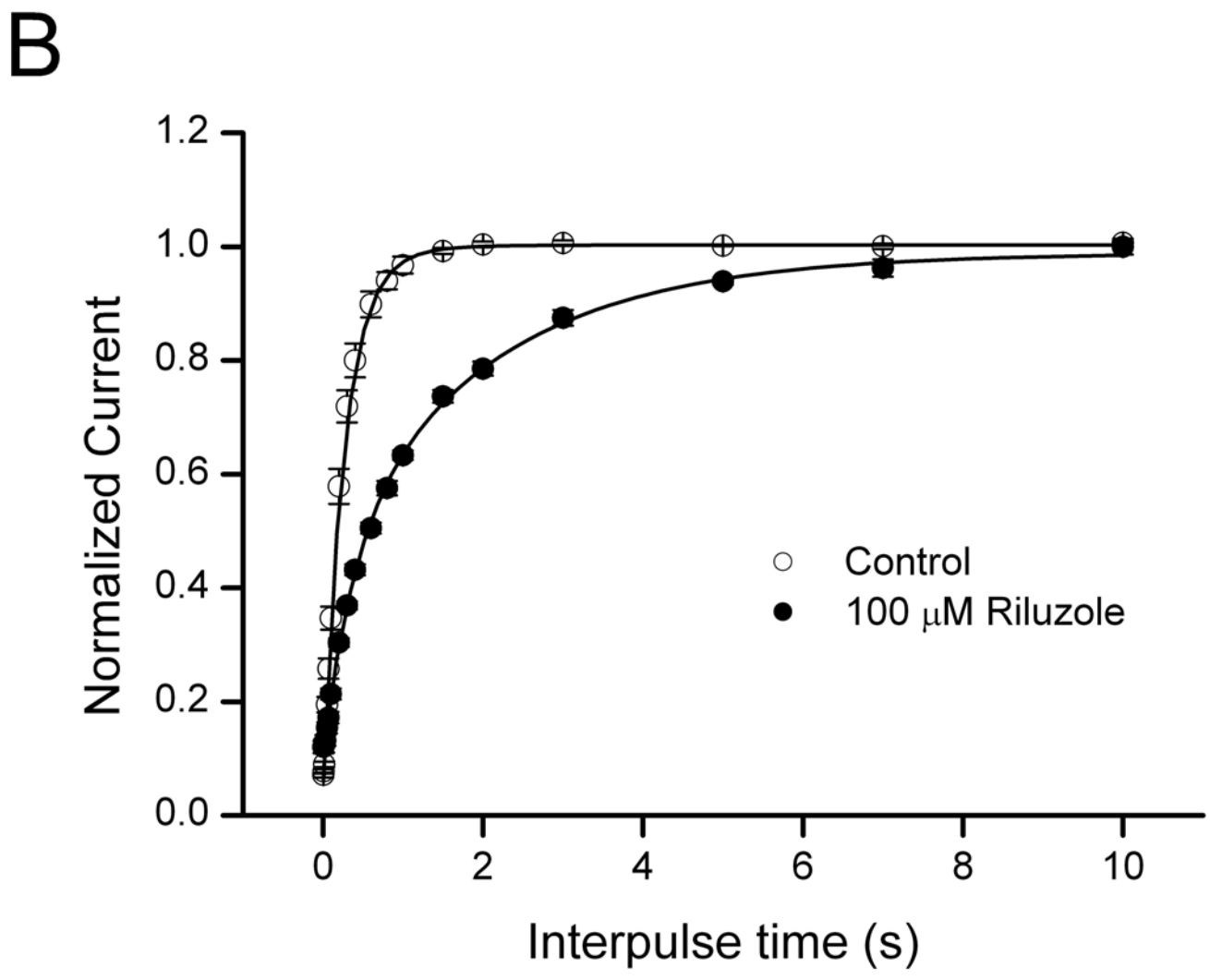

JPET Fast Forward. Published on June 30, 2006 as DOI: 10.1124/jpet.106.106724
This article has not been copyedited and formatted. The final version may differ from this version.